

A Hybrid Domain Approach to Remove Horizontal Stripping in Remote Sensing Images using Spatial, Frequency & Wavelet Components

Vikash Tyagi*, N Ravi, Wagh Ganesh Nana, P Suresh Kumar, & R Chandrakanth

ADRIN, Secunderabad, India

*Corresponding author's email: vikash@adrin.res.in

Abstract

Most of the remote sensing images contain stripes even after Non-Uniformity Correction. Stripes may be due to response of bad/degraded detector, differential variations in detector sensitivity to perceived energy, temperature variations. Stripes can occur in vertical or horizontal direction. In this paper, we are targeting horizontal stripes as these stripes degrades image quality & risks image suitability for analysis of various application like SR (Spectral Reflectance) generation, Spectral Signature extraction, classification etc. Even sometimes the visual interpretation also becomes difficult, if the width of stripes is continuous and wider. Hence, Horizontal destripping is an essential preprocessing step to achieve accurate results for classification and spectral based applications. There are many algorithms available in spatial domain like interpolation, filtering etc. But the spatial domain methods can correct horizontal stripes up to limited pixel lines effectively, beyond that there may be visual and spectral disturbances. With spectral domain method like spectral distance approach, results can be noisy due to multiple pixels that may have same spectral distance. In this paper, we proposed a Hybrid Domain Approach which incorporate advantages of spatial, wavelet & frequency domains methods. In spatial domain, width of horizontal stripes is estimated using dark pixel information followed by slope method for removing stripes. However, some residual horizontal stripes still remain in the image which is to be corrected by taking advantage of wavelet transform and Fast Fourier Transform. Wavelet transform as a multi-resolution representation of the image that has the ability to separate directional(horizontal) wavelet components at different scale levels. Horizontal wavelet components related to residual horizontal stripes are filtered with an adaptive filter in frequency domain. An inverse Fourier transform is applied to form de-striped wavelet component followed by inverse wavelet transform to reconstruct final de-striped image. After analysis with quantitative metrics such as Signal to Noise Ratio, Peak Signal to Noise Ratio and Root Mean Square Error, it has been found out that hybrid domain approach gives better results than existing methods. The results are presented in the paper.

Keywords Horizontal stripping, spatial components, frequency components, wavelet components

Introduction

Stripes lead to significant radiometric uncertainties in reflectance and radiance data. Hence, without correction, stripes are creating problems in higher-level remote sensing applications such as the normalized difference vegetation index, land surface temperature, classification, target detection etc [1, 2]. Remote sensing images contain stripes which affect the quality of

the image. Stripe occurs due to differential sensitivities of the detector elements to incoming radiation. The stripes affect the visual effect and quantitative interpretability. The stripes have different characteristics based on the scanning instrument. Push broom type imaging instruments are designed to acquire complete rows of images using a linear CCD (Charge Coupled Device) array placed across track [3]. Whiskbroom instrument obtain the image by scanning forward and backward across-track using all the detectors at a time [4]. If one detector of an array has a slightly modified or unbalanced responsivity from that of its neighbours or from its normal conditions resulting in a vertical column stripe and Horizontal stripe occur due to detector dynamic behaviour of CCD (Charged Coupled Device) caused by electronics & temperature variations. The nonlinear stripes are those whose degradation parameters change with the ground objects, and the irregular stripes are those in which only some of the pixels are contaminated. Periodic stripes are caused by poor radiometric calibration of the relative gain and offset of the individual detectors of the acquisition system. The deviation between the input/output transfer function of neighbouring elements of detector matrix remain constant with time. Periodic stripes originate in fine variation in the width of the slit. Random stripes are caused by thermal noise or random fluctuations in the sensor response. This type of disturbance results in bright and dark stripes with random length across the track. Due to stripes the result of various post processing operation will become vague for example if images contain stripe and classification operation is performed then one class related to stripe will occur. Stripe can be found out automatically by dark pixel (if certain threshold of dark pixel is present in column whose radiance value is less than the local neighbourhood pixels), by computing mean and variance of the row and by grey threshold method. The correction of image stripes is commonly known as image destripping.

In recent decades, many destripping techniques had been proposed and divided into digital filtering-based methods, statistics-based methods and optimization-based methods. Filtering based methods removes the stripes of remote sensing image by designing filter in transformed domain, such as Fourier Transform [5] which used to process the image data with a low pass filter using Discrete Fourier Transform, the advantage of this method is that it is useable on geo-rectified image, but it does not remove all stripes and can lead to significant blurring within the image. Wavelet Analysis [6] remove stripes by taking advantage of the scaling and directional properties to detect and eliminate striping patterns. Filtering based methods assume that stripping is periodic in nature and can be observed in power spectrum of the image. But the filter used to eliminate stripes may affect the spatial details with the same frequencies as stripes related to useful signal may result in blurring or ringing artefacts of destripped images.

To remove the limitation of blurring or ringing artefact researchers had gradually turned to statistical methods which depends on the statistical characteristics of the digital number of each image [7]. These algorithms examine the distribution of digital numbers for each image and adjusts this distribution to some reference distribution. Statistical-based methods have certain assumptions and are limited by image size, terrain distribution, and other conditions. Histogram matching [8] assumes that the histogram of each column in the image has the same distribution. Moment matching [9] assumes that the standard deviation and mean value of each column in the image are the same. If the image size is too small or the terrain difference is too large, these statistical-based methods cannot achieve satisfactory results. The destripping effect of statistical-based methods depends on the

universality and rationality of their assumptions. Since the assumption of moment matching is more general, its processing effect will be better than histogram matching.

Optimization-based destripping methods regard the stripe noise removal issue as an ill-posed inverse problem [10-13]. To find a better solution, prior knowledge of the ideal image is used to regularize the destripping problem. Introducing prior information, an estimation of the desired image can be computed by minimizing an energy function under a constrain term. In [10], Shen and Zhang proposed a maximum a posterior framework based on Huber-Markov regularization for both destripping and inpainting problems. Considering stripe noise has a clear direction signature, Bouali and Ladjal [11] developed a sophisticated unidirectional total variation (TV) model for stripe noise removal in MODIS (Moderate Resolution Imaging Spectroradiometer) data. Many researchers have proposed some improved unidirectional TV models by using different regularization [12-17]. Chang et al. [12] considered a combined unidirectional TV and frame regularization method for stripe noise removal as well as preserving more details. Zhang et al. [13] proposed a unidirectional TV-Stokes model, which avoids excessive over-smoothing by distinguishing stripe regions and stripe-free regions. In addition, for destripping of multispectral and hyperspectral images, researchers had taken full advantage of the high spectral correlation between the images in different bands [17-19]. In [18], the authors proposed the graph-regularize Low-Rank Representation (LRR) for destripping of hyperspectral images.

Although the above-mentioned methods have achieved satisfactory destripping results, they implement the destripping by directly estimating statistics of the desired images while ignoring the characteristics of stripe noise, which often causes damages to the image details along with the stripes. Relationship between DN (Digital Number) and Radiance remain linear but due to high resolution of the image relationship between DN (Digital Number) and Radiance become non-linear as different range of gray values can have different offsets and slopes as shown in Figure 1. In this paper to deal with nonlinear relationship and preserving the image details we have proposed hybrid domain approach to remove horizontal destripping from the image by combining dark pixel information from the sensor followed by Wavelet and Fourier transforms. Section 2 presents background related to Fourier and Wavelet transforms. Section 3 presents the proposed method for elimination of horizontal stripe. Section 4 presents the Experiment and Results. Section 5 presents the Conclusion.

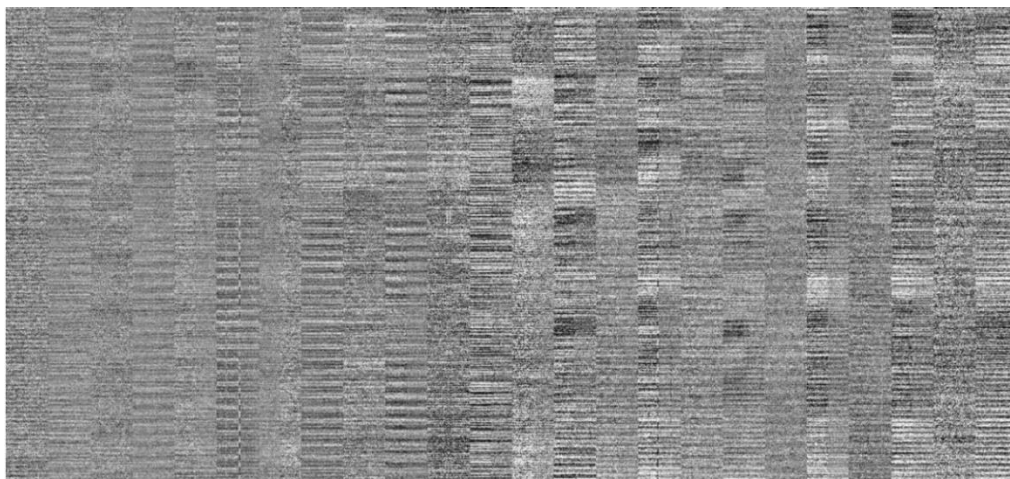


Fig. 1 Varying intensity of horizontal stripes in multispectral image.

Background

One of the motivations behind this research is to develop filtering algorithms that can efficiently minimize stripes and noise in high-resolution multispectral images (resolution is less than 2 metre). This type of noise occurs in the image acquisition direction (across direction) and is non-periodic in nature. Wavelet transform, as a multi-resolution and scale-space representation of the image, has the ability to separate directional stripe in certain directional wavelet components at different scale levels. On the other hand, Fourier transform can analyse image stripe in the frequency domain. As these transforms were incorporated in our proposed method, basic concepts of these transforms and their application in image filtering are reviewed in this section.

Fourier Transform: Fourier transform decomposes the signal into an infinite set of sinusoidal waves of different frequencies, amplitudes and phases. It transforms the image from spatial domain to frequency domain entirely. The first component corresponds to the zero-frequency value that is the mean amplitude of the signal, also known as the Direct Current (DC)[20]. For analyzing a discrete signal, Discrete Fourier Transform (DFT), which represents a finite sum of sinusoidal functions, is used. One-dimensional DFT is mathematically expressed in [Equation (1)] where the complex exponential term represents the sum of sine and cosine terms and 'i' is imaginary number. F_k is known as Fourier coefficient.

$$F_k = \sum_{n=0}^{N-1} x_n e^{-\frac{2\pi i}{N}kn} \quad k = 0, 1, \dots, N - 1 \quad \text{Eq. 1}$$

Fourier transform generates real and imaginary components and can also be represented by amplitude and phase components. DFT is invertible and the image can be perfectly reconstructed using the Inverse Discrete Fourier Transform (Inverse DFT) expressed in equation (2):

$$x_n = \sum_{k=0}^{N-1} F_k e^{\frac{2\pi i}{N}kn} \quad n = 0, 1, \dots, N - 1 \quad \text{Eq. 2}$$

DFT can be easily expanded to two dimensions (2-D) or multidimensions by composing sequences of one-dimensional DFTs along each dimension in any order. 2-D DFT is expressed in equation 3 where F_{kl} , known as the Fourier coefficient, is the complex amplitude of component x_{kl} .

$$F_{kl} = \sum_{n=0}^{N_x-1} \sum_{l=0}^{N_y-1} f_{mn} e^{-j2\pi(\frac{mk}{N_x} + \frac{nl}{N_y})} \quad \text{Eq. 3}$$

Image stripes are condensed in the frequency domain to a narrow central band of high amplitude values in a direction orthogonal to the stripes. For instance, vertical stripes are presented as a horizontal central narrow band in Fourier domain. Filtering in Fourier transform involves examining and locating noise frequency components in the transform power spectrum, designing a blocking filter to remove them, applying the filter on the image spectrum and inverting back to image domain to obtain the de-noised image [20]. One of the advantages of image filtering in the frequency domain is the capability to implement the

filter as a simple multiplication. Different types of Fourier filters have been proposed [21] [22] [23] to filter out the stripe frequencies in the frequency domain. These types of Fourier transform filtering can be categorized into hard mask filtering, such as box or rectangular mask, and soft mask filtering, such as Gaussian notch filter. Most of the Fourier filtering methods have been successfully tested in filtering images with periodic stripes. However, many of these methods require some manual input in developing filter masks, and, in the case of non-periodic stripes, loss and distortion of image information can occur. In our proposed method, we applied an adaptive Fourier filtering scheme that normalizes the DC term of individual rows of the wavelet components of the image dominated by the stripe noise.

Wavelet Transform:

Wavelet transform represents any arbitrary function as a superposition of wavelets [23]. Unlike Fourier transform, wavelet transform retains both spatial and frequency information. Wavelet transform utilizes narrow groups of wavelets of different shapes (e.g. Debauchies, Morlet, Haar, Mexican Hat, etc.) that represent local and non-periodic patterns of a signal better than Fourier transform [24]. Unlike the continuous sinusoidal wave function that Fourier uses a wavelet is a brief oscillation function that is localized in space. Wavelet transform is used in multi-resolution analysis to obtain different approximations of a signal function $f(x)$ at different levels of resolution. For continuous wavelet transform, wavelet coefficient is attained by:

$$W_{a,b} = \frac{1}{\sqrt{a}} \int f(x)\psi_{a,b}(x)d(x) \tag{Eq. 4}$$

where a and b are scale and translation parameters along x -axis. And function of transform or admissible wavelet is obtained by scaling and translation of a mother wavelet $\psi(x)$.

$$\psi_{a,b} = \psi\left(\frac{x-b}{a}\right) \tag{Eq. 5}$$

In discrete signal and according to the dyadic sampling, a and b are considered 2^j and $k2^j$, respectively. Then the wavelet function on an orthonormal basis is defined as:

$$\psi_{j,k}(x) = 2^{-\frac{j}{2}}\psi(2^{-j}x - k) \tag{Eq. 6}$$

Where, j and k determine the position and width of wavelet along the x -axis. In multi-resolution analysis, a scaling function $\varphi(x)$ is used to create a series of approximations of the function; each differs by a factor of 2 in resolution. Wavelet functions $\psi(x)$ are then used to encode the difference in information between approximations [24]. Wavelet function can be expressed as a weighted sum of shifted, double-resolution scaling function:

$$\psi(x) = \sum_n h_\psi(n)\sqrt{2}\varphi(2x - n) \tag{Eq. 7}$$

Where, the $h_\psi(n)$ are called the wavelet function coefficients. The scaling function coefficient $h_\psi(n)$ can be related h_φ to by the equation $h_\psi(n) = (-1)^n h_\varphi(1 - n)$. Fast Wavelet Transform (FWT) [25] algorithm for fast and efficient implementation of Discrete Wavelet Transform (DWT) is based on the relationship between the coefficients of the

DWT at adjacent scales. Detail coefficient (W_ψ) and approximation coefficient (W_φ) at scale $j + 1$ can be derived as:

$$W_\psi(j, k) = \sum_m h_\psi(m - 2k)W_\varphi(j + 1, m) \quad \text{Eq. 8}$$

$$W_\varphi(j, k) = \sum_m h_\varphi(m - 2k)W_\varphi(j + 1, m) \quad \text{Eq. 9}$$

These equations show that both the approximation and detail coefficients at scale j can be obtained by convolving $W_\varphi(j + 1, k)$, approximation coefficient at the scale $j + 1$, with the reversed scaling and wavelet vectors, $h_\varphi(-n)$ and $h_\psi(n)$ followed by the subsequent subsampling. In one-dimensional (1-D) multi-resolution analysis, signal $f(x)$ is decomposed into an approximation (low pass) and a detail (high pass) component in one scale level. After decomposition, the size of these components is halved by down-sampling. The approximation component can undergo iterative decomposition in the next scale level. The theory of multi-resolution analysis and wavelength can be extended to 2-D or higher dimensions. Two-dimensional wavelet transform is a multi-resolution, scale-space representation of 2-D data, such as digital images. It is represented by one scaling function and three directionally sensitive wavelet functions at each scale level.

$$\varphi(x, y) = \varphi(x)\varphi(y) \quad \text{Scaling function} \quad \text{Eq. 10}$$

$$\psi^H(x, y) = \psi(x)\varphi(y) \quad \text{Wavelet horizontal function} \quad \text{Eq. 11}$$

$$\psi^V(x, y) = \varphi(x)\psi(y) \quad \text{Wavelet Vertical function} \quad \text{Eq. 12}$$

$$\psi^D(x, y) = \psi(x)\psi(y) \quad \text{Wavelet Diagonal function} \quad \text{Eq. 13}$$

Where, $\varphi(x, y)$ represents the scaling function and $\psi^H(x, y)$, $\psi^V(x, y)$, and $\psi^D(x, y)$ represents directional wavelet functions in horizontal, vertical and diagonal directions, respectively.

Two-dimensional wavelet transform (decomposition) can be obtained by taking the 1-D DWT of the rows of the signal data $f(x, y)$ and the subsequent 1-D DWT of the resulting columns. In a signal scale process, four quarter-size sub-images, one approximation coefficient (W_φ) and three sets of detail coefficients ($W\psi^H$, $W\psi^V$ and $W\psi^D$) are produced. The approximation coefficient, W_φ , is further decomposed at the next scale level. In multi-resolution scale levels, the signal is decomposed into one approximation coefficient at the lowest frequency level and three detail coefficients at each of the scale levels. In each scale level, these three detail coefficients $W\psi^H$, $W\psi^V$ and $W\psi^D$ captures the horizontal variations (horizontal stripes, edges), vertical variations (vertical stripes, edges) and the variations along the diagonal directions, respectively.

Wavelet capability of decomposing an image into directional detail components in multiple scale levels is advantageous in detecting and eliminating stripes. Sidelstripes separate out in detail coefficients of corresponding direction. Non-periodic directional stripes have different frequencies and appear at many scale levels. Filtering out stripes from these directional wavelet components is more effective than filtering out stripes directly from original image. Generally, wavelet-based image filtering is performed in three main steps: (i) decomposition of image into wavelet components in specified scale levels; (ii)

treatment of the striped directional components; and (iii) image reconstruction from filtered components.

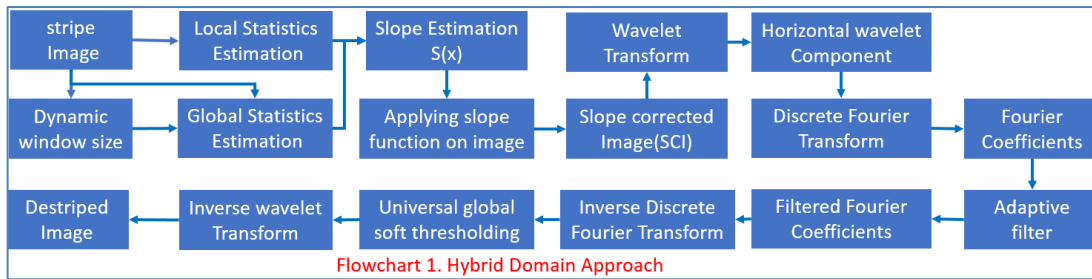
Despite efficiency in stripe detection, wavelet-based filtering is still complicated by the fact that directional components also capture non-stripe signals, including contrasting feature edges in addition to the stripes. Non-stripe signals become more significant at higher scale (lower frequency) levels and blend with stripe information complicating the filtering algorithm, which limits the efficiency of wavelet-based filtering in reducing non-periodic stripes.

Proposed Method:

Our de-stripping method is based on a combination of dark pixel slope estimation, wavelet decomposition and frequency domain adaptive filtering. In spatial domain, width of horizontal stripes is estimated using dark pixel information followed by slope method for removing horizontal stripes. However, some residual horizontal stripes still remain in the image which is to be corrected by taking advantage of wavelet transform and FFTs. Slope corrected image is decomposed into wavelet components in a given number of scale levels. The wavelet directional components related to residual horizontal stripes are filtered with an adaptive filter in the frequency domain. Discrete Fourier transform (DFT) is applied on individual rows (along stripe direction) of the stripe-rich wavelet components. An adaptive filter is applied by detecting and excluding potential non-stripe extreme pixels and normalizing the DC values adaptively in order to suppress the stripe effect only. An inverse Fourier transform is then applied to form the de-striped wavelet component at each level, followed by inverse wavelet transform to reconstruct the final de-striped image. We are discussing each individual step in further details in subsections.

Dark Pixel Slope Estimation:

Multispectral imaging consists of certain number of devices. Each device consists of definite number of ports. Each port contains image data as well as dark pixel (which has correlation information with respect to width of horizontal stripes). The main reason for using dark pixel is that the width size of horizontal stripe in high resolution multispectral image is dynamic. Multispectral sensor contains dark pixel which is very useful for the calculation of the window size for applying first order statistics to remove horizontal stripe in the images. We have applied dark pixel slope on multispectral images port wise. Multispectral image contains one dark pixel for each port. There are two methods for calculation of the window size, by calculating the difference between the adjacent trough (or crest) of the dark pixel vs pixel number curve as shown in Figure 2. In this method the window size is dynamic and it changes for every row. For every row there is a different reference statistics estimation and local first order statistics for removing stripe. Slope for each row is calculated by dividing the reference mean by local mean for that row. Slope is applied on each row to get slope corrected image after which Wavelet and Fourier transforms are applied to remove horizontal residual stripes. The whole procedure is explained in the flow chart {1}.



Wavelet and Fourier Transforms:

The slope corrected image is subjected to Discrete Wavelet Transform (DWT) and decomposed into a number of frequency scale levels. At each level, three directional components (horizontal, vertical and diagonal) are formed in addition to the image approximation component. This process separates the stripes (in addition to other image contents) in the detail wavelet components in the stripe direction (e.g. horizontal stripes in the horizontal detail components). Non-periodic stripes, as in multispectral imagery captured by push broom sensors, appear in a number of scale levels. For most wavelet implementation, determining the wavelet type [wavelet type=Daubechies(db4)] and number of scale levels (level used for this experiment is 3) is an experimental step that varies according to the residual stripe and image characteristics. Horizontal wavelet components are transformed to the frequency domain using 1-D Fourier transform.

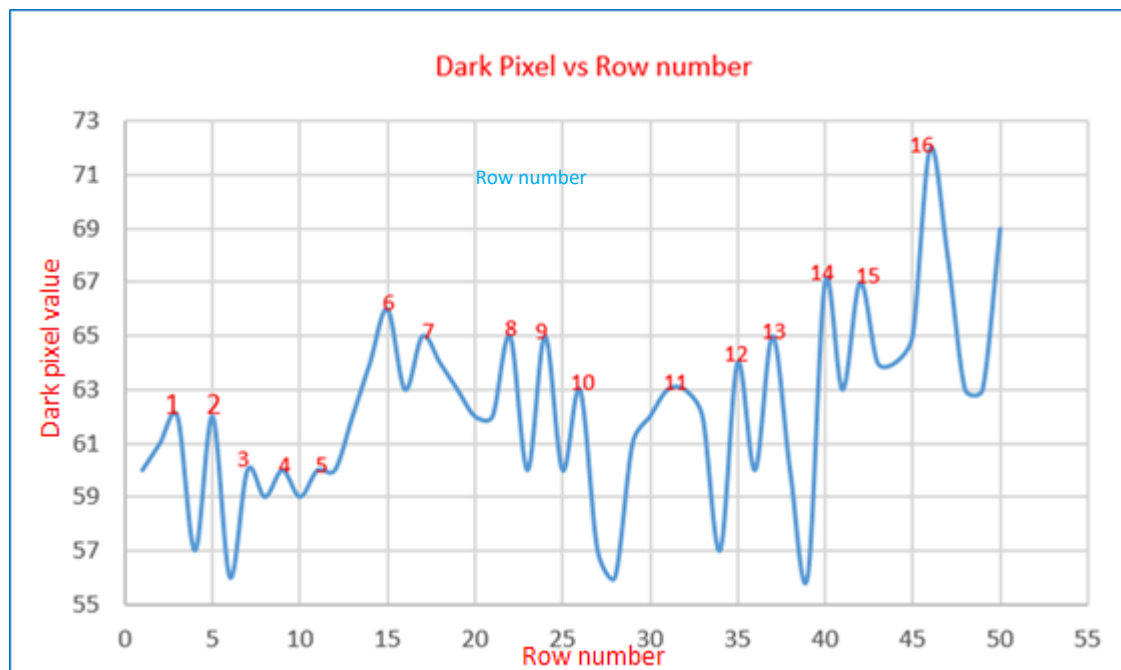


Fig. 2 Plot of dark pixel and row number to find out different crest/trough location.

The components are transformed as individual vectors, where each vector contains the digital numbers of a single row. We are filtering individual rows in the horizontal component of the image wavelet transform. This process emphasizes the stripes in the frequency domain as variations in the DC (Direct Current or, amplitude value of the zero-frequency) values of the Fourier transform of individual row. Generalized frequency filtering can be used at this point to de-stripe the residual striped horizontal wavelet components by

equalizing the DC value of each row Fourier transform. One of the approaches that can be used to perform such normalization is to set the DC values to zero (or any constant value). The DC value represents the mean amplitude of the signal row and is proportional to the row mean in the spatial domain. Equalizing the DC values in this sense can introduce artifacts, especially for small images and for images with highly contrasting features. Edges of such features (non-stripe features) appear in the horizontal wavelet components can influence the algorithm. Results may have less striping, however, smearing artifacts will be introduced due to the effect of the DC equalization process that will change values in the original image so that the average of each row's values will be the same. To overcome this problem, we introduced an adaptive filter that detects and accounts for influential non-stripe signals in the horizontal wavelet component when normalizing the DC values in the frequency domain. Influential pixel values (e.g. high-contrast feature edges) in the horizontal wavelet components are detected in each row along the striping direction as those beyond a specific statistical threshold from the row neighbourhood mean. A new vector X^j as shown in equation (14) free from these pixels is created by excluding influential values from the original wavelet vector so that

$$x_i^j \in y^j \text{ if } (x_i^j - X^j) < k * \sigma \quad \text{Eq.14}$$

Where, x_i^j is the value for pixel i in row j, X^j is the statistical mean of the digital numbers of row j (or few rows adjacent to row j), σ is the standard deviation of the wavelet component, k is a coefficient threshold used to set the filtering value as a multiplier of the standard deviation σ . In our method, three parameters (wavelet type, number of scale levels "L", and threshold value "k") need to be determined based on the image content and stripe characteristics. The final normalized DC value for each row as shown in equation (15) can be computed as proportional to the difference of the mean before and after excluding influential signal values and is computed as follows:

$$F_{norm}^j = F_{orig}^j * \frac{X^j - Y^j}{X^j} \quad \text{Eq.15}$$

Where, F_{orig} and F_{norm} are the DC values of the Fourier Transform of the original and normalized column, respectively, and Y^j is the mean of the column after excluding influential signal. Note that if there are no values related to high-contrast features in the wavelet directional component columns, the final DC value F_{norm} is zero; otherwise, the final normalized DC value will be raised or lowered accordingly. Wavelet details component is subject to a soft thresholding process, where the detail value is set to zero if it is less than a certain threshold determined from image noise level.

Detailed steps of proposed Method:

Step 1: Compute local statistic(mean) of each row in input image as shown in equation (16) where N is the total number of columns.

$$R_i = \frac{\sum_{j=0}^N I(i,j)}{N} \quad \text{Eq. 16}$$

Step 2: Estimate dynamic window size for each row by calculating forward trough location (ftl) & backward trough location (btl) based on dark pixel estimation as shown in equation (17)

$$dws_i = (ftl - btl) * NF \quad \text{Eq. 17}$$

where, NF is normalization factor. For example, we have to estimate window size for scan line 4, we have to locate forward trough (i.e. 2 in figure 2) and backward trough (i.e. 1 in figure 2), the difference between forward trough location and backward trough location is (5-3) =2 which is multiplied by default normalization factor=4 resulting in window size of 8 for scan line 4. The normalization factor can vary from 2 to 6.

Step 3: Compute global statistic (gs) for each row of input image as shown in equation (18) where N is the total number of columns, dws represent dynamic window size.

$$gs_i = \frac{\sum_{k=i-dws_i}^{k=i+dws_i} \sum_{j=0}^N I(k,j)}{N*dws} \quad \text{Eq. 18}$$

Step 4: Estimation of slope (sl) for each row of input image as shown in equation (19)

$$sl_i = \frac{gs_i}{R_i} \quad \text{Eq. 19}$$

Step 5: Apply slope on each row of input image to obtain Slope Corrected Image (SCI) as shown in equation (20) to remove horizontal stripe. But some residual stripe still remains in the image which is removed using wavelet and Fourier transform.

$$SCI = I(i, j) * sl_i \quad \text{Eq. 20}$$

Step 6: Estimate different directional component of image using Debauchies wavelet transform as shown in equation (21) & in figure 3 where AC denote Approximation Coefficients, HD denote horizontal details, VD denote vertical details and DD denote diagonal detail of the image.

$$AC, HD, VD, DD = DWT(SCI) \quad \text{Eq. 21}$$

Step 7: Estimating influential pixel vector (ipv) (e.g. high-contrast feature edges) as shown in equation (14) in the horizontal wavelet components in each row along the striping direction as those beyond a specific statistical threshold from the row neighborhood mean.

Step 8: Estimating Fourier Transform of row vector of horizontal wavelet component as shown in equation (22) & in figure 4 after excluding influential pixel vector.

$$Row_i = FT(row_i - ipv_i) \quad \text{Eq. 22}$$

Step 9: Normalizing DC component of Row vector by difference of mean before and mean after excluding influential pixel vector as shown in equation (15).

Step 10: calculate Inverse Fourier transform to obtain residual horizontal stripe free wavelet component as shown in equation (23).

$$row_i = IFT(ROW_i)$$

Eq. 23

Step 11: Replace modified horizontal wavelet component in wavelet coefficients with universal soft thresholding and apply inverse wavelet transform to obtain residual horizontal stripe free image.

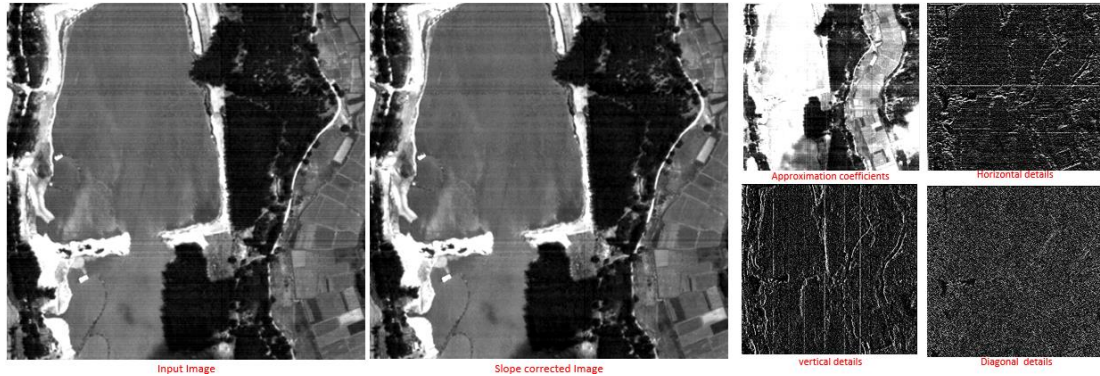


Fig. 3 Input image, slope corrected image & wavelet component of slope corrected image as approximation coefficients, horizontal, vertical & diagonal details.

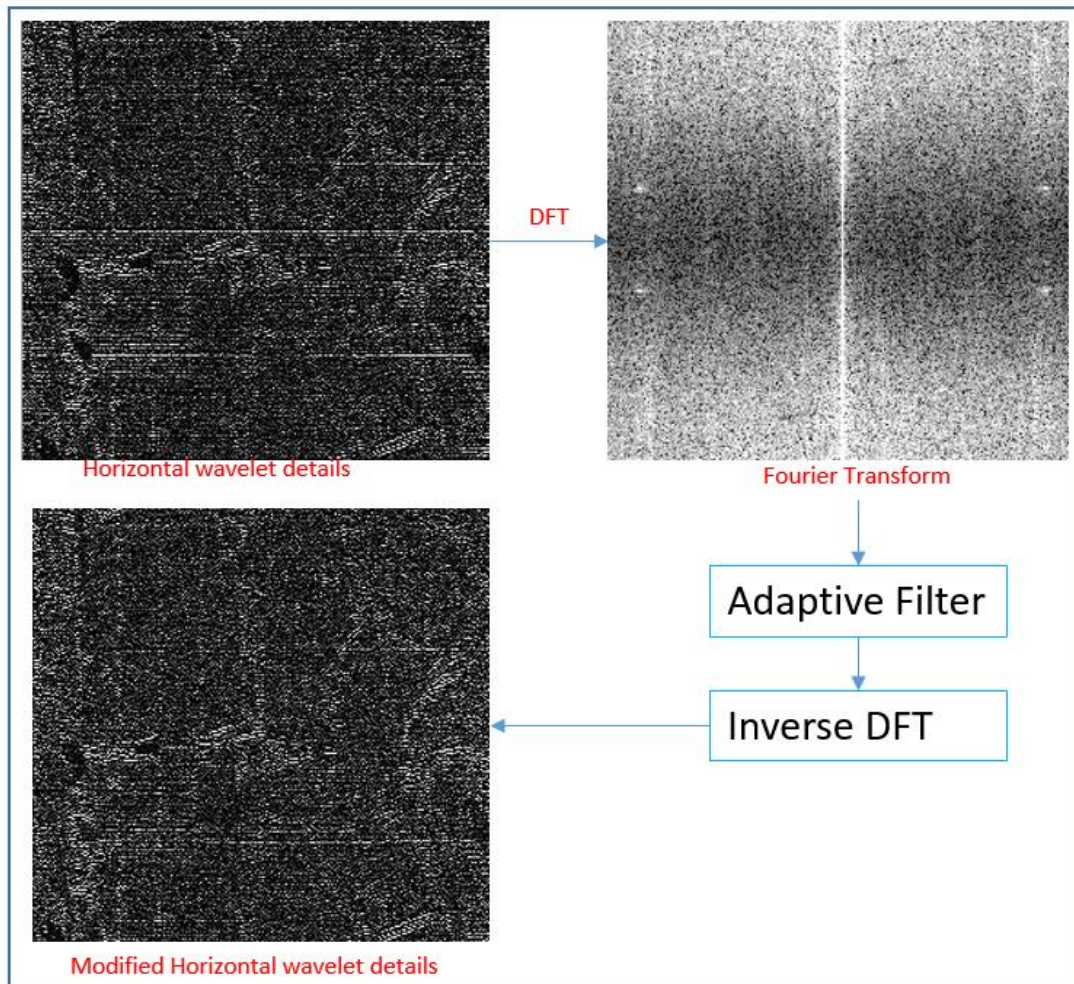


Fig. 4 showing result of Fourier transform on horizontal wavelet details and result of adaptive filter on Fourier coefficients to obtain modified horizontal wavelet details.

Experiment and Results

We have tested the proposed method using various sets of high-resolution multispectral image (resolution is less than 2 meter) which include variety like water, cloud, vegetation etc. Before applying the proposed method, different methods to remove noise were applied like ghost noise removal & adaptive noise removal. We have made out a comparison between the result of Mean offset, Mean slope, Fourier Transform, Wavelet Transform and hybrid domain method. Figures 5, 6 & 7 represent comparison output of different methods.

Visual Inspection: Visual assessment constitutes a primary step in assessing the quality of multispectral images and selecting the bands suitable for analysis. Extending visual assessment to evaluate the quality of image de-stripping and to help determine de-stripping parameters is not new to the multispectral image processing community. In this research, the de-striped images resulting from applying different methods were visually assessed and compared. Mean offset method depend on the calculation of the reference mean and row mean in image across the track. The main parameter is reference mean. Reference mean can be global mean (mean of the whole image), window mean (mean of local area, window of 100 or any other size), device mean (mean of the pixels of the device of the image; number of pixels in the device may vary on the sensor characteristics). In Mean slope method, slope for each row is calculated by dividing the reference mean by the row mean. The reference mean can be global mean or local mean. Then each pixel is updated by multiplying the pixel with its respective row slope. Slope method gives good results than offset method. In Fourier Transform image is transformed to Fourier domain where DC component of each row is replaced with mean of row excluding DC component followed by inverse Fourier Transform to obtain destriped Image. In Wavelet Transform Image is transformed to different wavelet component in which Horizontal component is modified by using slope method followed by Inverse Wavelet Transform to obtained destriped Image. Figure 5 shows the result of different methods when applied on image which contain vegetation. In case of vegetation, Mean Offset, Mean Slope, Fourier Transform (modified spectral property of image as color change of features is observed) & Wavelet Transform (introduce dotted artifact in image) methods were not able to remove stripes as hybrid domain method perfectly removed horizontal stripes. Figure 6 shows result on homogenous image, mean offset method introduce artifacts in darker region due to overall statistics of the image, while mean slope method also failed to remove stripes, Fourier Transform (modified spectral property of image as color change of features is observed), Wavelet Transform (introduce dotted artifact in image) while hybrid domain method removed horizontal stripes in homogenous image. Figure 7 shows the result on heterogeneous image which contain vegetative and water, mean offset and slope methods tried to introduce artifacts in vegetation areas due to statistics of water region, Fourier & Wavelet Transform change the spectral property of features in image but hybrid domain method removed horizontal stripes without introducing any artifact in heterogeneous image while preserving spectral property of feature in image. For all tested images, differences in filtering quality resulting from the implementation of different filtering methods were clear and could be compared visually.

Quantitative assessments

Multispectral high-resolution Images are used for Quantitative assessment with parameters like Signal to Noise Ratio (SNR), Peak Signal to Noise Ratio (PSNR) & Root Mean Square Error (RMSE) which quantify image filtering quality [26] [27]. SNR, which is commonly used as a measure of signal (or image) quality, is computed as the ratio of mean value of a signal to the standard deviation of a signal as expressed in the equation (24) below:

$$SNR = \left(\frac{Mean}{standard\ deviation} \right) \tag{Eq. 24}$$

Table 1 compare the SNR of Mean offset, Mean slope, Fourier Transform, Wavelet Transform method & Hybrid Domain Approach and it has been found out that SNR value is high after processing image with hybrid domain approach.

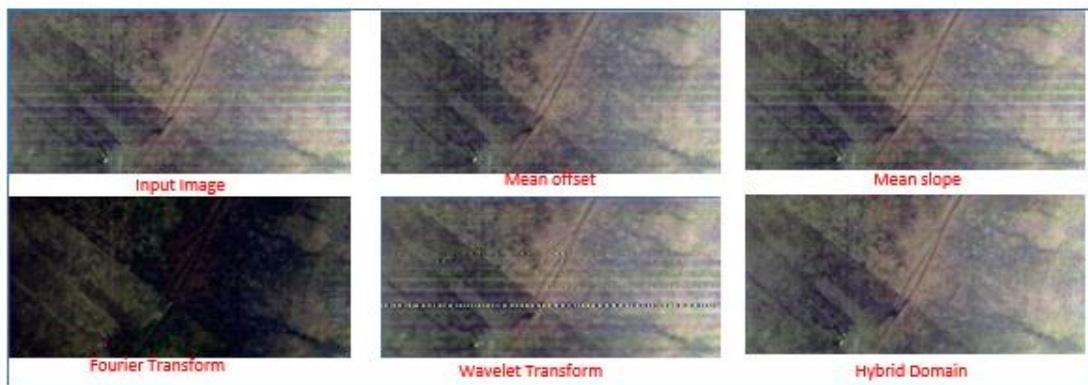


Figure 5

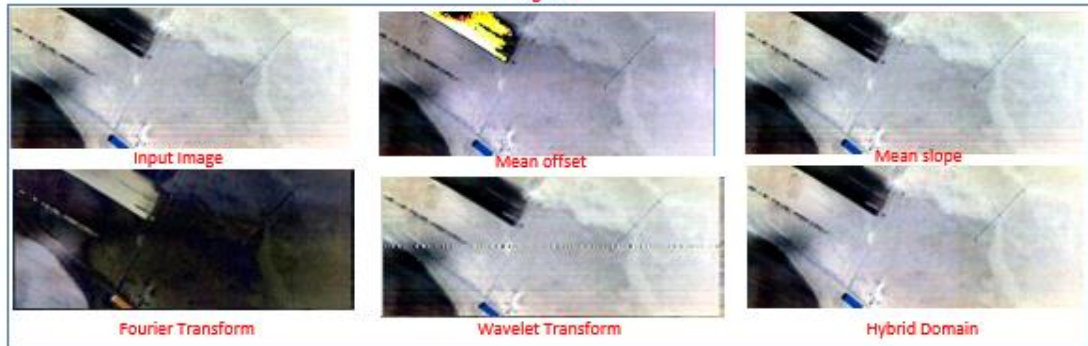


Figure 6

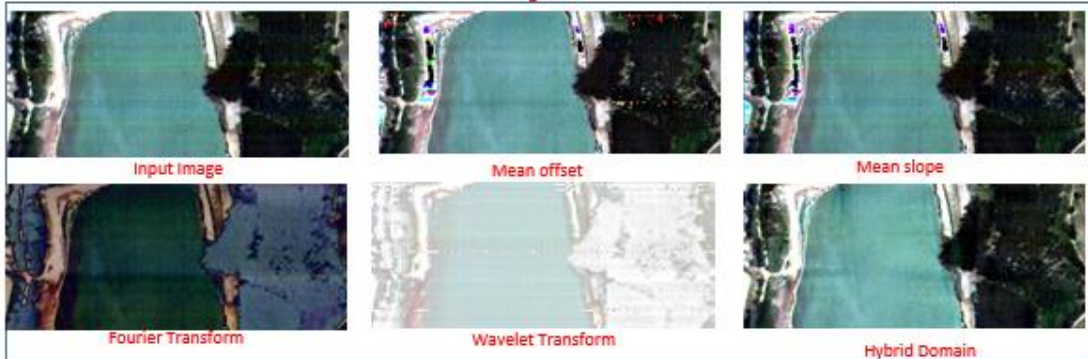


Fig. 7 Comparisons of differ outputs.

Table 1 SNR values of different methods.

Image \SNR	Input Image	Mean offset	Mean slope	Fourier Transform	Wavelet Transform	Hybrid Domain
Image1	3.06	3.12	3.1	1.56	2.94	3.15
Image 2	2.009	2.006	2.02	1.08	2.66	2.2
Image 3	5.65	10.52	6.33	1.62	1.39	6.6

RMSE is used as an image noise measure and can be conveniently computed as in equation (25):

$$RMSE = \sqrt{\frac{1}{M*N} \sum \sum [(p(i,j) - q(i,j))^2]} \quad \text{Eq. 25}$$

Where, M and N refer to the image number of rows and columns, respectively; p(i, j) and q(i, j) are the pixel value at row i and column j for the clean and processed image respectively.

Table 2 RMSE value of different methods.

Image \ RMSE	Mean offset	Mean slope	Fourier Transform	Wavelet Transform	Hybrid Domain
Image1	8.01	9.37	10.49	10.39	5.3
Image 2	7.07	6.74	10.71	6.06	5.24
Image 3	9.15	5.79	10.65	5.27	4.8

Table 2 represent RMSE value comparisons and it has been found out that RMSE value for hybrid domain method is lower than Mean offset, Mean slope, Fourier Transform & Wavelet Transform method. PSNR (Peak Signal to Noise Ratio) is used as a measure of image quality, is computed as the ratio of maximum possible power of a signal to the power of corrupting noise and expressed in logarithmic decibel scale as expressed in equation (26):

$$PSNR = 10. \log_{10}(MAX^2 / MSE) \quad \text{Eq. 26}$$

Where, MAX is the maximum possible value (e.g. 255 for 8-bit image) and MSE is the Mean Squared Error. Table 3 represent PSNR value computed from various methods. PSNR value of Hybrid Domain method is higher than Mean offset, Mean slope, Fourier Transform & Wavelet Transform method.

Table 3 PSNR of different methods.

Image \ PSNR	Mean offset	Mean slope	Fourier Transform	Wavelet Transform	Hybrid Domain
Image1	28.65	29.65	27.75	27.74	31.19
Image2	28.64	29.45	27.78	30.84	29.56
Image3	28.94	30.47	27.88	30.84	32.4

Conclusion

In this study, we introduced the Hybrid Domain Approach based on dark pixel slope estimation, wavelet multi-resolution image analysis and adaptive Fourier transform filtering. The method separates residual image stripes using wavelet decomposition and adaptively normalizes the zero-frequency components of individual vectors (rows) in the direction of the stripes. The adaptive nature of the hybrid domain method removes the artifacts that could occur in small-sized images or in the case of the existence of contrasting features. We also tested Mean offset, Mean slope, Fourier Transform & Wavelet Transform method. We applied the quantitative assessment using RMSE, SNR & PSNR on the input images and on processed images. Our comparison showed that the proposed Hybrid Domain Approach de-stripping algorithm performed excellently when applied to all images, which was shown visually and evidenced by the quantitative assessment results.

Future work: In this study we have focused on horizontal stripe present in an image but there is other oblique stripe as well as noise present in the image. In future study we will try to remove different directional stripe as well as noise using Hybrid Domain Approach based on different mother Wavelet testing and different type of adaptive filters to be incorporated in Fourier domain.

References:

1. Zhang, H.; Li, J.; Huang, Y.; Zhang, L. A nonlocal weighted joint sparse representation classification method for hyperspectral imagery. *IEEE J. Sel. Topics Appl. Earth Observ. Remote Sens.* 2014, 7, 2056–2065.
2. Stein, D.W.; Beaven, S.G.; Hoff, L.E.; Winter, E.M.; Schaum, A.P.; Stocker, A.D. Anomaly detection from hyperspectral imagery. *IEEE Signal Process. Mag.* 2002, 19, 58–69.
3. Yuhengchen, Yiqun Ji, Jinakong Zhou, Xinhua chen, Wei Xiaoxiao, Weimen shen “Distortion measurement of pushbroom imaging spectrometer”. *Proceeding of SPIE November 2009*, volume 7506,211-219
4. James Edwin Fowler “Compressive pushbroom and whiskbroom sensing for hyperspectral remote sensing imaging”. 2014 IEEE International conference on Image Processing,684-688.
5. Chen, J.; Chang, C. Destripping of Landsat MSS images by filtering techniques. *Photogramm. Eng. Remote Sensing* 1992, 58, 1417–1423.
6. Torres, J.; Infante, S.O. Wavelet analysis for the elimination of striping noise in satellite images. *Opt. Eng.* 2001, 40, 1309–1314.
7. Sun, L.; Neville, R.; Staenz, K.; White, H.P. Automatic destripping of Hyperion imagery based on spectral moment matching. *Can. J. Remote Sens.* 2008, 34, 68–81.
8. Acito, N.; Diani, M.; Corsini, G. Subspace-based striping noise reduction in hyperspectral images. *IEEE Trans. Geosci. Remote Sens.* 2011, 49, 1325–1342.
9. Weinreb, M.; Xie, R.; Lienesch, J.; Crosby, D. Destripping GOES images by matching empirical distribution functions. *Remote Sens. Environ.* 1989, 29, 185–195
10. Shen, H.; Zhang, L. A MAP-based algorithm for destripping and inpainting of remotely sensed images. *IEEE Trans. Geosci. Remote Sens.* 2009, 47, 1492–1502.
11. Bouali, M.; Ladjal, S. Toward optimal destripping of MODIS data using a unidirectional variational model. *IEEE Trans. Geosci. Remote Sens.* 2011, 49, 2924–2935.

12. Chang, Y.; Fang, H.; Yan, L.; Liu, H. Robust destriping method with unidirectional total variation and framelet regularization. *Opt. Express* 2013, 21, 23307–23323.
13. Zhang, Y.; Zhou, G.; Yan, L.; Zhang, T. A destriping algorithm based on TV-Stokes and unidirectional total variation model. *Optik-Int. J. Light Electron Opt.* 2016, 127, 428–439.
14. Zhou, G.; Fang, H.; Lu, C.; Wang, S.; Zuo, Z.; Hu, J. Robust destriping of MODIS and hyperspectral data using a hybrid unidirectional total variation model. *Optik-Int. J. Light Electron Opt.* 2015, 126, 838–845.
15. Chang, Y.; Yan, L.; Fang, H.; Liu, H. Simultaneous destriping and denoising for remote sensing images with unidirectional total variation and sparse representation. *IEEE Geosci. Remote Sens. Lett.* 2014, 11, 1051–1055.
16. Wang, M.; Zheng, X.; Pan, J.; Wang, B. Unidirectional total variation destriping using difference curvature in MODIS emissive bands. *Infrared Phys. Technol.* 2016, 75, 1–11.
17. Acito, N.; Diani, M.; Corsini, G. Subspace-based striping noise reduction in hyperspectral images. *IEEE Trans. Geosci. Remote Sens.* 2011, 49, 1325–1342.
18. Lu, X.; Wang, Y.; Yuan, Y. Graph-regularized low-rank representation for destriping of hyperspectral images. *IEEE Trans. Geosci. Remote Sens.* 2013, 51, 4009–4018.
19. Chang, Y.; Yan, L.; Fang, H.; Luo, C. Anisotropic spectral-spatial total variation model for multispectral remote sensing image destriping. *IEEE Trans. Image Process.* 2015, 24, 1852–1866.
20. Schowengerdt, R.A., 2007. *Remote Sensing: Models and Methods for Image Processing*, third ed. Academic Press, pp. 229–354.
21. Liu, J.G., Morgan, G.L.K., 2006. FFT selective and adaptive filtering for removal of systematic noise in ETM+ imageodesy images. *IEEE Transactions on Geosciences and Remote Sensing* 44 (12), 3716–3724.
22. Zhang, Z., Shi, Z., Guo, W., Huang, S., 2006. Adaptively image destriping through frequency filtering. In: *ICO 20: Optical Information Processing.*, Proceedings SPIE, vol. 6027, Changchun, China, August 21–26, pp. 989–996.
23. Antonini, M., Barlaud, M., Mathieu, P., Daubechies, I., 1992. Image coding using wavelet transform. *IEEE Transactions on Image Processing* 1 (2), 205–220.
24. Gonzalez, R.C., Woods, R.E., 2008. *Digital Image Processing*, third ed. Pearson Prentice Hall, pp. 461–524.
25. Mallat, S.G., 1989. A theory for multiresolution signal decomposition: the wavelet representation. *IEEE Transactions on Pattern Analysis and Machine Intelligence* 11 (7), 674–693.
26. Eskicioglu, A.M., Fisher, P.S., 1995. Image quality measures and their performance. *IEEE Transactions on Communication* 43 (12), 2959–2965.
27. Huynh-Thu, Q., Ghanbari, M., 2008. Scope of validity of PSNR in image/video quality assessment. *Electronics Letters* 44 (13), 800–801.

Citation

Tyagi, V., Ravi, N., Nana, W.G., Kumar, S.P., Chandrakanth, R. (2024). A Hybrid Domain Approach to Remove Horizontal Stripping in Remote Sensing Images using Spatial, Frequency & Wavelet Components. In: Dandabathula, G., Bera, A.K., Rao, S.S., Srivastav, S.K. (Eds.), *Proceedings of the 43rd INCA International Conference, Jodhpur, 06–08 November 2023*, pp. 351–366, ISBN 978-93-341-2277-0.

Disclaimer/Conference Note: The statements, opinions and data contained in all publications are solely those of the individual author(s) and contributor(s) and not of INCA/Indian Cartographer and/or the editor(s). The editor(s) disclaim responsibility for any injury to people or property resulting from any ideas, methods, instructions or products referred to in the content.